

Structure, Stability, and Quantum Conductivity of Small Diameter Silicon Nanowires

Inna Ponomareva,^{1,*} Madhu Menon,^{2,†} Deepak Srivastava,^{3,‡} and Antonis N. Andriotis^{4,§}

¹*Department of Physics, University of Arkansas, Fayetteville, Arkansas 72701, USA*

²*Department of Physics and Astronomy and Center for Computational Sciences, University of Kentucky, Lexington, Kentucky 40506, USA*

³*NASA Ames Center for Nanotechnology, UARC, MS 229-1, Moffett Field, California 94035-1000, USA*

⁴*Institute of Electronic Structure and Laser, Foundation for Research and Technology-Hellas,*

P.O. Box 1527, Heraklio, Crete, Greece 71110

(Received 18 April 2005; published 20 December 2005)

Structures and energetics of various types of silicon nanowires have been investigated using both quantum and classical molecular dynamics simulations to determine the most stable forms. The tetrahedral type nanowires have been found to be the most stable and, surprisingly, the polycrystalline forms of nanowires, while having the smallest surface to bulk ratio, are found to be the least stable. We also show that the cagelike nanowires have greater thermal stability than the tetrahedral nanowires. Furthermore, their electrical conducting properties are found to be better than those of tetrahedral nanowires, suggesting useful molecular electronic applications.

DOI: [10.1103/PhysRevLett.95.265502](https://doi.org/10.1103/PhysRevLett.95.265502)

PACS numbers: 61.46.+w, 68.65.-k

The field of low dimensional semiconductor structures is very attractive due to its tremendous technological potential. The current interest in silicon nanowires (Si-NWs) is an offshoot of this phenomenon. Various methods have been used to fabricate Si-NWs. They include the laser ablation method [1,2], the oxide assisted catalyst-free method [3,4], and solution techniques [5]. The Si-NWs produced using these methods come in various diameters and are usually covered with an oxide sheet. In a significant recent development, experimentalists have succeeded in removing this oxide sheet and terminating the surface with hydrogen [6]. Most of these wires consist of a single crystalline core.

Some possible structures for Si nanowires have been predicted recently [7–11]. In works reported in Refs. [7,8] nanowires consist of fullerenelike cages. In particular, the Si-NW structures proposed by Menon and Richter [7] have fourfold coordinated cores and threefold coordinated surfaces with one of the most stable reconstructions of bulk Si. Such reconstruction is of great importance since it provides a reduction in the surface energy that can be relatively high for quasi-one-dimensional structures, especially in the small diameter regime. Recently, Zhao *et al.* [10] have compared the energetics of formation of Si-NWs with crystalline and polycrystalline cores and suggested that for very thin (1–3 nm) nanowires, polycrystalline maybe a valid candidate for the lowest energy structure.

Despite these recent reports, an exhaustive stability analysis by a consideration of a large number of Si-NWs to determine the most stable geometry is currently lacking. In the absence of any direct experimental evidence for the structure of thin nanowires, there could be several competing structures with energetics and stabilities close to each other. Although the diamond structure (tetrahedral) is established to be the most stable form of bulk Si, the clathrate

or cagelike forms of bulk Si are very close in energies to the diamond structure. In the case of small diameter Si-NWs, however, the possibility exists that the relatively larger contribution of surface energies could tilt the balance in favor of either the clathrate or the polycrystalline forms. The small diameter Si-NWs exhibit direct band gaps [7,12] and show great promise in optoelectronics applications. A knowledge of their precise structure would be very useful in the determination of their optoelectronics properties. A thorough energetic analysis of a wide variety of Si-NW structures using reliable theoretical methods by incorporating a careful consideration of surface reconstructions is, therefore, very timely.

In this Letter we present a systematic study of the stability analysis of Si-NWs by considering tetrahedral, cagelike, as well as polycrystalline wires. All the smaller diameter nanowires (≤ 6 nm) were fully relaxed without any symmetry constraints using the generalized tight-binding molecular dynamics (GTBMD) scheme of Menon and Subbaswamy [13]. This scheme has been successfully used in obtaining geometries and vibrational properties of various bulk phases of Si as well as Si clusters of arbitrary sizes [13,14]. All the Si-NWs were taken to be of infinite length and modeled by large supercells incorporating a constant pressure (“movable wall”) ensemble [15]. This allows for a simultaneous relaxation of lattice and basis degrees of freedom. A uniform grid consisting of 126 k points was used in the calculation of forces. A total of 65 Si-NWs were considered. All nanowires had crystalline cores consisting of fourfold coordinated atoms and threefold coordinated surface atoms. Surface reconstructions for all structures were obtained carefully. The GTBMD calculations were complemented by molecular dynamics simulations using the Stillinger-Weber (SW) many-body potential [16]. This scheme was used to perform simulations for Si-NWs in the range 1–15 nm. The SW inter-

atomic potential consists of two- and three-body interaction terms and was originally fitted to describe the crystalline and liquid silicon phases. For very thin Si-NWs the surface to volume ratio is expected to be very large and the energetics from the classical SW potential may not be very accurate as compared to the energetics and stability analysis with the quantum GTBMD method. A combination of the two approaches has allowed us to test the structural stability and energetics of various Si-NWs as a function of diameter.

The nanowires considered belonged to four different categories, with Fig. 1 showing a representative for each type for very narrow diameters. The cagelike Si-NWs used in this work were carved out from Si clathrate structures consisting of a face centered cubic (fcc) lattice with a 34 atom basis (Si_{34} -Clath) as well as a simple cubic (sc) lattice with a 46 atom basis (Si_{46} -Clath) [17]. Both these clathrate forms are known to be the most stable clathrate forms for bulk Si. The cohesive energies for the bulk tetrahedral, Si_{34} -Clath and Si_{46} -Clath, obtained using the SW potential are, respectively, 4.34 eV, 4.30 eV, and 4.29 eV. The corresponding values obtained using the GTBMD method are 5.27 eV, 5.24 eV, and 5.23 eV, respectively. The energetic ordering of these structures is identical to that obtained using first principles methods [18]. Furthermore, the relative energies are also very close to the first principles values. The growth direction for the tetrahedral wires is taken to be along the $\langle 111 \rangle$ direction. In addition to tetrahedral and clathrate wire forms, which both belong to single crystalline category, we also considered polycrystalline nanowires [10]. The polycrystalline structure is essentially tetrahedral in nature with stacking fault type grain boundaries as defects.

In Fig. 2, we show the diameter dependence of the cohesive energy for the Si-NWs obtained using the GTBMD scheme for the fully relaxed nanowires of diameter up to 5 nm. As seen in the figure, single crystalline nanowires of both tetrahedral and cagelike forms are found

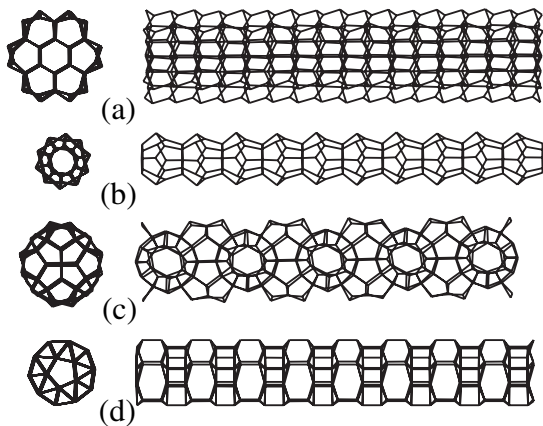


FIG. 1. Figure showing a representative set of small diameter Si-NWs consisting of (a) tetrahedral, (b) Si_{34} -Clathrate, (c) Si_{46} -Clathrate, as well as (d) polycrystalline types of nanowires.

to be more stable than the polycrystalline ones, with stacking fault type grain boundaries, for all small diameter nanowires. Furthermore, among the single crystalline Si-NWs, the tetrahedral form is found to be the most stable, followed by the Si_{34} -Clath and Si_{46} -Clath, respectively, indicating that the energetic ordering of bulk fourfold coordinated Si structures is also maintained for nanowire forms. We have also performed molecular dynamics and energetics simulations for the nanowires in the larger diameter range (1–15 nm) using the classical SW potential. The results are shown in the inset of Fig. 2. In the larger diameter range of 2–15 nm, SW potential results are in agreement with the more accurate GTBMD method and support the finding that both the tetrahedral and clathrate type of single crystalline nanowires are more stable than the polycrystalline nanowires. For diameters less than 1.8 nm, the polycrystalline nanowires are found to be unstable under the SW potential and collapse into lower symmetry structures whose energies are shown by the dotted line in the inset of Fig. 2. Interestingly, there is a crossover of this dotted line with the lines for single crystalline structures, suggesting that at very small diameters the collapsed polycrystalline wires may have lower energies than the single crystalline wires. It should be noted, however, that at such small diameters quantum effects are significant and classical potentials cannot be relied on to provide a correct description of the energetics of these nanowires. This can be seen from the qualitatively different results obtained in the GTBMD calculations that shows the single crystalline nanowires to be more stable for all diameters.

The above stability analysis is further investigated by plotting the cohesive energies of the nanowires as a function of their surface to volume ratio in Fig. 3. The surface to

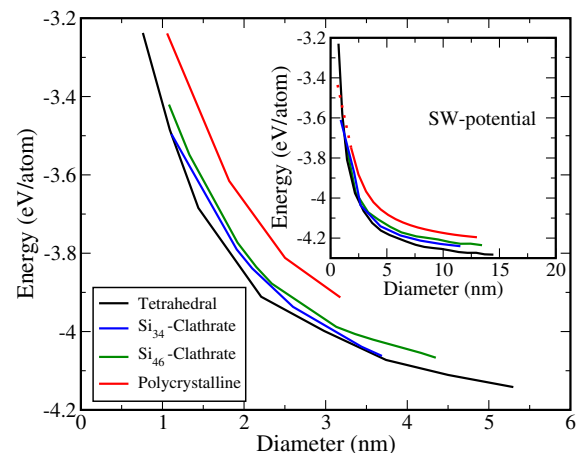


FIG. 2 (color online). Plot showing the diameter dependence of the cohesive energy for the Si-NWs obtained using the GTBMD scheme for the fully relaxed nanowires. The inset shows the corresponding dependence obtained using the classical SW many-body potential. Both methods show the tetrahedral wires to be the most stable and polycrystalline to be the least stable.

volume ratio is qualitatively represented by the ratio of surface type atoms (with threefold coordination) to bulk type atoms (with fourfold coordination). The upper left panel of Fig. 3 shows results obtained using the SW potential for the larger diameter range, while the GTBMD results for the smaller diameter range are shown in the upper right panel. The dependence of surface to volume ratio on the nanowire diameter is shown in the lower left panel of Fig. 3. As shown in the figure, for the same diameter, the surface to volume ratio of the polycrystalline nanowires in all the cases are smaller than the surface to volume ratio of the single crystalline nanowires of the tetrahedral and clathrate types. This is expected because the formation of stacking fault type defects in polycrystalline structures with pentagonal cross section minimizes the surface to volume ratios for a given diameter. Furthermore, the difference in the surface to volume ratio between the polycrystalline and single crystalline structures increases significantly for the wire diameters of less than 0.5 nm. The total cohesive energies, including the contributions from the bulk, surface, and stacking fault defect type atoms, as function of surface to volume ratio, therefore, are valid criteria for comparing the stability of these structures. The cohesive energies as a function of surface to volume ratio (see Fig. 3) show the increasing instability of the polycrystalline structures for higher surface to volume ratio or smaller diameter nanowires of up to ≈ 1.8 nm diameter. For diameters ≤ 1.8 nm, the polycrystalline structures, as noted above, are not stable with either the SW potential or the GTBMD method and collapse into

mixed configurations with no clear distinction between surface and bulk type atoms. For the same surface to volume ratio, an examination of the cohesive energies show the single crystalline nanowires of tetrahedral and clathrate type structures to be significantly more stable than the polycrystalline wires. It should also be noted that the novel chemical, mechanical, electronic, and optoelectronic properties expected in the higher surface to volume ratio materials will be possible for single crystalline structures and not as much for polycrystalline structures which have been predicted through bulklike analysis [10] which may not be valid in nanoscale materials.

The temperature dependent stability analysis of these nanowires is carried out next. In this case, the potential energy function of the four types of nanowires of diameter ≈ 4.5 nm and surface to volume ratio between 0.12–0.18 were computed in molecular dynamics simulations with SW potentials and shown in the lower right part of Fig. 3. We use an Evans-Hoover thermostat for finite temperature simulations [19,20]. The temperature was varied and raised up to over 3000 K. The polycrystalline wire was found to have the least temperature dependent stability when compared to those of crystalline tetrahedral and clathrate type structures. As seen in Fig. 3, the slopes remain constant until melting for single crystalline nanowires, while the slope is irregular for the polycrystalline nanowire. An examination of the polycrystalline structure revealed that in the center of the nanowire, an amorphouslike core begins to develop near 250 K. As the temperature increases, the amorphous region expands exclusively through one of the five facets, engulfing it entirely at ≈ 500 K. The amorphous region then expands to include other facets while the slope remains approximately constant until melting. The temperature analysis further confirms the instability of the polycrystalline nanowires whose melting temperature of 1250 K is significantly lower than those of the single crystalline nanowires. In the case of single crystalline nanowire, melting first occurs for tetrahedral nanowire at around 1500 K. Surprisingly, the clathrate nanowires show more durability when subjected to heating with a melting temperature of 1760 K for the Si_{34} -Clath. The higher melting point for the clathrate type wires can be understood by a careful examination of the structures just prior to melting. The melting is seen to start from the surface and the surface of Si_{34} wire, which has the highest melting point, is more stable under heating since it has mostly closed cages on the surface, unlike the case of tetrahedral or even Si_{46} wires. The melting curves for bulk tetrahedral Si as well as bulk Si_{34} -Clath are also shown in the figure for comparison. The melting temperature of 2000 K for the bulk tetrahedral structure obtained in our simulations is higher than the experimental value of 1600 K. It should be noted, however, that experimental samples almost always contain defects and impurities that act to lower the melting temperature. The melting temperature for bulk Si_{46} -Clath is obtained to be 2000 K, the same as that for the bulk tetrahedral phase. An interesting

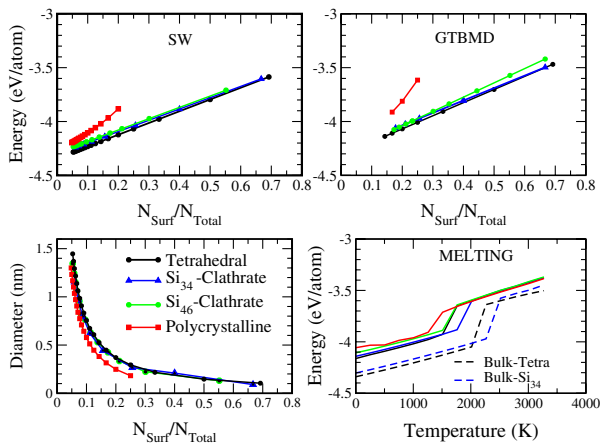


FIG. 3 (color online). Cohesive energies of Si-NWs obtained in relation to their surface to volume ratio using the SW potential (upper left panel) and the GTBMD method (upper right panel). The legends for all four panels are indicated in the lower left panel which also shows the relationship between the surface to volume ratio and the nanowire diameter. The surface to volume ratio of polycrystalline nanowires in all cases are smaller than the corresponding ratio for the single crystalline nanowires. The temperature dependent stability of the different types of Si-NWs is shown in the graph on the lower right panel which also includes the melting curves for bulk tetrahedral as well as the bulk Si_{34} clathrate structure for comparison.

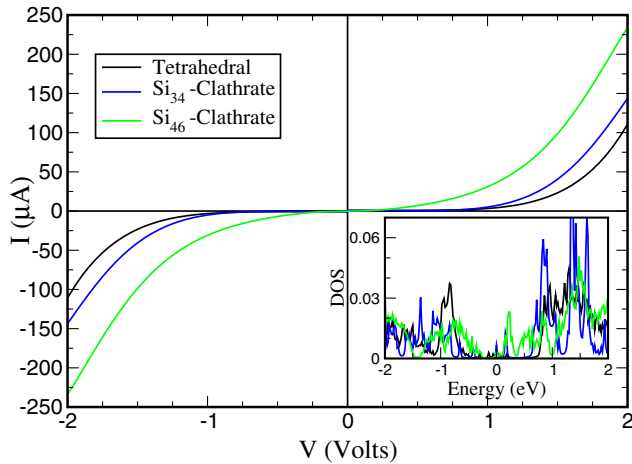


FIG. 4 (color online). Current vs voltage (I - V) characteristics for the single crystalline nanowires of tetrahedral and cagelike geometries obtained under symmetric bias. The inset shows the densities of states (DOS) for the same nanowires. The Fermi level is at $E = 0$. Both cagelike crystalline nanowires show better conducting properties than the tetrahedral nanowire under low bias.

point of observation is that the energetic ordering is maintained for all nanowires up to the melting temperature. We, however, note that the melting curves in Fig. 3 were computed in constant volume simulations and hence represent only a qualitative description of the melting behavior of different types of Si-NWs. The complete phase diagrams at different constant pressures could be simulated in the future to quantify the melting of different silicon nanowires described in this work.

We investigate the quantum conductivity of various nanowires next. In Fig. 4 we present the calculated I - V curves for the single crystalline nanowires of tetrahedral and cagelike geometries obtained under symmetric bias. The inset shows the densities of states (DOS) for the same nanowires. There were no hydrogens attached to the surface atoms which were allowed to relax naturally. The wires are of finite length (4–9 nm) and the Si atoms at both ends were passivated with hydrogen. The conductivity is calculated using a formalism incorporating the transfer Hamiltonian approximation (THA) method [21] in which the bias-voltage is applied self-consistently (to be referred to as the SC-THA method). The Hamiltonian used in the SC-THA method is the *same* as used in performing the GTBMD structural relaxation for the Si-NWs. This allows for consistency in our calculations. Interestingly, the cagelike nanowires, and, in particular, the Si_{46} clathrate nanowires, perform better under low bias voltage when compared to the tetrahedral nanowires. An examination of the DOS in the inset reveals the transport gap to be largest for the tetrahedral nanowire and smallest for the Si_{46} -Clath nanowire. The narrowing of the transport gap results in the conductivity increase for the clathrate nanowires. This

could have important technological implications when these nanowires are used in device applications.

In summary, we have presented results for stability and conductivity for different Si-NWs. Our results show that the polycrystalline forms of nanowires, while having the smallest surface to bulk ratio, are also the least stable. Our results also show that the cagelike nanowires have higher melting temperatures and, therefore, greater thermal stabilities than the tetrahedral nanowires. Furthermore, their electrical conductivity is found to be better than tetrahedral nanowires.

The present work is supported through grants by NSF (ITR-0221916), DOE (00-63857), KSTC (03-66986), and US-ARO (W911NF-05-1-0372). Part of this work (D. S.) is supported by NASA Contract No. NAS2-03144 to UARC.

*Electronic address: iponoma@uark.edu

†Electronic address: super250@pop.uky.edu

‡Electronic address: deepak@nas.nasa.gov

§Electronic address: andriot@iesl.forth.gr

- [1] Y.F. Zhang, Y.H. Tang, N. Wang, D.P. Yu, C.S. Lee, I. Bello, and S.T. Lee, *Appl. Phys. Lett.* **72**, 1835 (1998).
- [2] A.M. Morales and C.M. Lieber, *Science* **279**, 208 (1998).
- [3] N. Wang, Y.H. Tang, Y.F. Zhang, C.S. Lee, I. Bello, and S.T. Lee, *Chem. Phys. Lett.* **299**, 237 (1999).
- [4] J.L. Gole, J.D. Stout, W.L. Rauch, and Z.L. Wang, *Appl. Phys. Lett.* **76**, 2346 (2000).
- [5] J.D. Holmes, K.P. Johnston, R.C. Doty, and B.A. Korgel, *Science* **287**, 1471 (2000).
- [6] D.D.D. Ma, C.S. Lee, F.C.K. Au, S.Y. Tong, and S.T. Lee, *Science* **299**, 1874 (2003).
- [7] M. Menon and E. Richter, *Phys. Rev. Lett.* **83**, 792 (1999).
- [8] B. Marsen and K. Sattler, *Phys. Rev. B* **60**, 11 593 (1999).
- [9] B. Li, P.C.R.Q. Zhang, and S.T. Lee, *Phys. Rev. B* **65**, 125305 (2002).
- [10] Y. Zhao and B.I. Yakobson, *Phys. Rev. Lett.* **91**, 035501 (2003).
- [11] M. Menon, D. Srivastava, I. Ponomareva, and L.A. Chernozatonskii, *Phys. Rev. B* **70**, 125313 (2004).
- [12] X. Zhao, C.M. Wei, L. Yang, and M.Y. Chou, *Phys. Rev. Lett.* **92**, 236805 (2004).
- [13] M. Menon and K.R. Subbaswamy, *Phys. Rev. B* **55**, 9231 (1997).
- [14] M. Menon, E. Richter, and K.R. Subbaswamy, *Phys. Rev. B* **56**, 12 290 (1997).
- [15] H.C. Andersen, *J. Chem. Phys.* **72**, 2384 (1980).
- [16] F. Stillinger and T. Weber, *Phys. Rev. B* **31**, 5262 (1985).
- [17] M. Menon, E. Richter, and K.R. Subbaswamy, *Phys. Rev. B* **56**, 12 290 (1997).
- [18] K. Moriguchi, S. Munetoh, and A. Shintani, *Phys. Rev. B* **62**, 7138 (2000).
- [19] W.G. Hoover, A.J.C. Ladd, and B. Moran, *Phys. Rev. Lett.* **48**, 1818 (1982).
- [20] D.J. Evans, *J. Chem. Phys.* **78**, 3297 (1983).
- [21] A.N. Andriotis, M. Menon, and D. Srivastava, *J. Chem. Phys.* **117**, 2836 (2002).